

Mechanical Characterization of Biofilms by Optical Coherence Elastography (OCE) Measurements of Elastic Waves

Hong-Cin Liou
Dept. of Mechanical Engineering
Northwestern University
Evanston, IL, USA
hc.liou@u.northwestern.edu

Fabrizio Sabba
Dept. of Civil and Environmental
Engineering
Northwestern University
Evanston, IL, USA
fabrizio.sabba@northwestern.edu

George Wells
Dept. of Civil and Environmental
Engineering
Northwestern University
Evanston, IL, USA
george.wells@northwestern.edu

Oluwaseyi Balogun
Dept. of Mechanical Engineering
Dept. of Civil and Environmental
Engineering
Northwestern University
Evanston, IL, USA
o-balogun@u.northwestern.edu

Abstract—Biofilms are biological materials composed of microbial communities encased in a self-produced extracellular polymeric substance (EPS). The viscoelastic properties of biofilms are related to the cross-link density in the EPS and ultimately the cohesiveness of biofilms. Accurate measurement of biofilm viscoelastic properties at the mesoscale remains a challenge. Rheological measurements, although being more common, provide only global properties, do not permit in-situ characterization, and are not amenable to complex sample geometries. To address these challenges, our work seeks to develop a nondestructive framework for characterizing biofilm viscoelastic properties using elastic wave propagation measured by the optical coherence elastography technique. The framework holds great potential to elucidate spatially varying mechanical properties and their correlation with sample morphology and composition.

Keywords—optical coherence elastography, nondestructive viscoelastic characterization, biofilm, elastic wave propagation

I. INTRODUCTION

Biofilms are biological materials composed of microbial communities encased in a self-produced extracellular polymeric substance (EPS). Among different phases of the microbial life, biofilm is the most dominant one in aquatic, sediment, and soil environments [1,2]. Biofilms can be beneficial or detrimental, depending on the types of microorganism and their function. An example for the former kind is the biofilms used to remove toxic substances in the wastewater, which is more environmentally friendly compared to the treatment processes that heavily depend on chemicals [3]. On the other hand, biofouling that sabotages the pipe systems or introduces unnecessary drag on maritime vehicles is an example for the latter kind [3]. In this context, the mechanical properties of biofilms have attracted great research interests for the potential to enhance or suppress certain kinds of biofilms in different applications. The mechanical properties are thought to be dependent on the morphology and composition in the biofilms, and may affect important processes such as formation, attachment, or

detachment, which are crucial for biofilms' explicit topology and functions [4].

Most approaches reported in the literature to characterize biofilm mechanical properties are based on macro- or micro-rheological techniques [5]. These techniques inherit some limitations due to the measurement length scale. For example, the macro-rheological measurements can only obtain bulk average of the characterized properties and are incapable of probing spatial variation in the biofilms. On the other hand, the micro-rheological ones only measure the properties that are highly localized, which are hard to be correlated with biofilms' morphology and compositional distribution that often fall in the $10^{-4}\sim 10^{-2}$ m scale (mesoscale). Moreover, both macro- and micro-rheological techniques are often destructive, creating large disturbance in samples, or required to be implemented *ex situ*. To address the challenges and fulfill the needs for mesoscale measurements, we have developed a mechanical characterization approach combining a wave propagation model and an imaging technique that can monitor the waves traveling in the sample. The imaging technique, termed as Optical Coherence Elastography (OCE), uses an Optical Coherence Tomography (OCT) microscope to map the elastography in biofilm samples. OCE can construct 3D nondestructive mapping of mechanical properties along with several exceptional characteristics such as (1) high imaging resolution at microscale, (2) high displacement sensitivity at nanoscale, (3) high sampling rate at 10~100 kHz, and (4) high compatibility to sample's geometry. These advantages prevent creating large disturbance in the samples, allow real-time monitoring, enable samples to be tested in their native environment (e.g. aquatic solution), and avoid geometric changes of the samples. Furthermore, the OCT image co-registered with the OCE image is an emerging handy tool to study the sample morphology and its relationship with the mechanical properties.

In this paper, we present the dispersion curves (frequency-dependent elastic wave speed) of a planar biofilm and a spherical biofilm (granular biofilm) measured by OCE technique. We also present two different guided elastic wave models with different geometries for theoretically predicting the dispersive relations in a layered plate and a layered cylinder. The prediction from the

This work was supported by the National Science Foundation via Award CBET-1701105 and the seed funding from the Department of Civil and Environmental Engineering at Northwestern University.

models will be used to estimate the viscoelastic properties of the biofilms through inverse analysis where the model calculations find the best fits to the experimental data. As we successfully applied this approach on the planar biofilm, the spherical biofilm requires additional information—especially the elastic property variation along the depth—to more precisely estimate the mechanical properties. To address this need, we developed a new technique that is capable of probing local elastic wave speed. The combination of all the approaches and techniques reported in this paper provides a promising framework toward nondestructive viscoelastic characterization on biofilms with various geometries.

II. METHODS

A. Image Acquisition Setup

Fig. 1 shows the schematic of the experimental setup for OCE measurements. Elastic waves are generated by the paddle actuator and monitored by the OCT microscope (Thorlabs GAN210C1, NJ, USA). The paddle actuator comprises a 10 mm wide razor blade, an 18-gauge syringe needle, and a piezoelectric transducer (Thorlabs PZS001). The piezoelectric transducer is driven by a radio frequency function generator (Agilent 33120, CA, USA) outputting single-frequency sinusoidal voltage, which creates oscillatory motion of the needle-blade assembly. The motion leads to a periodic indentation on the sample surface and generates harmonic compressional, shear, and surface elastic waves. The former two kinds of waves propagate into sample's interior region and, when encountering sample boundaries, are reflected back or transmitted into the surrounding environment. The surface waves travel within the near-to-surface region of the sample and exhibit frequency-dependent wave speed due to their varying penetration depth with frequency and finite sample thickness. The PC unit receives the data from the OCT and stores the acquired images for further post-processing. The synchronization device uses the TTL triggering signal from the function generator to synchronize the OCT scanning rate and the wave excitation frequency so that sample's dynamic responses induced by the harmonic wave can be visualized [6].

OCT microscope is an interferometer-based device using partially coherent laser light source to resolve the internal structure of partially transparent samples. It has two types of image output as shown in Fig. 2—the gray scale image (referred as OCT image) and the red-blue phase distribution (referred as OCE image). The former shows sample's morphology, and the red-blue pattern in the latter is correspondent to the dynamic responses. The contrast in the OCT image is related to the amount of back-scattered laser light from different depths in the sample. The laser light is scattered back due to the contrast of the refractive indices in the sample, which is dependent on

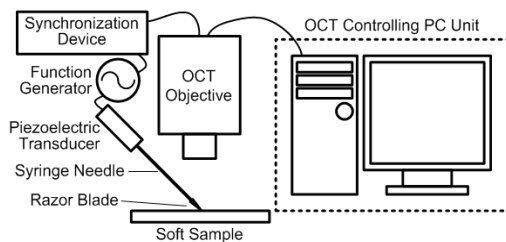


Fig. 1. Experimental setup for OCE measurements

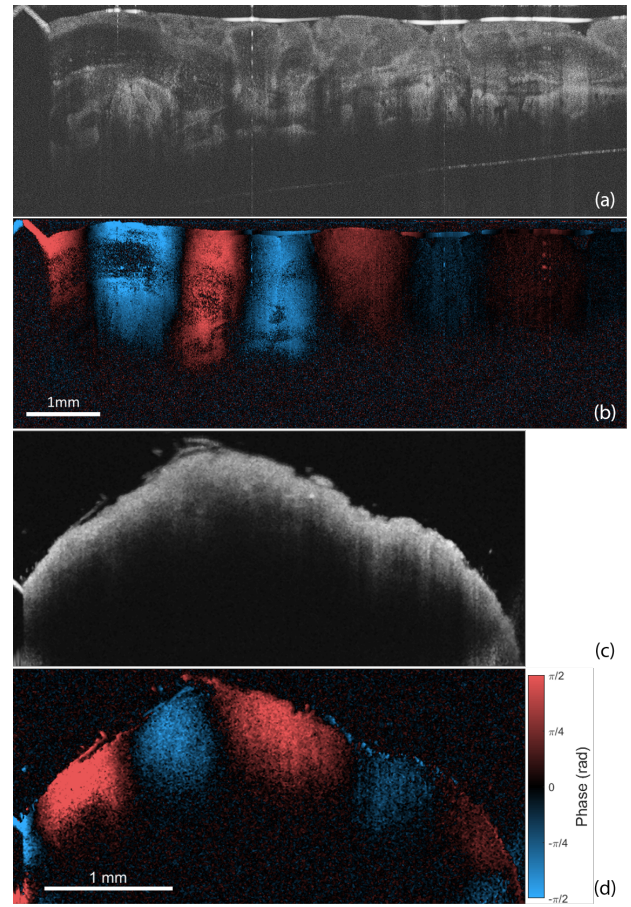


Fig. 2. OCT images (gray-scale) and OCE images (red-blue patterns) for planar biofilm (a and b) and granular biofilm (c and d).

sample's structural or compositional features. For example, in Fig. 2a, the bright lines on the top of the image corresponds to the biofilm-air interface and the dark bands correspond to pores. In Fig. 2c, the image has brighter intensity within the region close to the sample surface, but it decays strongly with depth. The abrupt intensity change is due to the penetration depth of the laser light, which depends on the optical properties of both the light source and the sample material. On the other hand, the red-blue color map in Fig. 2b and 2d is corresponding to the positive and negative values of phase difference $\Delta\phi$, which is an interferometer parameter and is related to the local displacement in the sample by the formula $\Delta\phi(x,z,t) = 4\pi n(x,z)\Delta u_z(x,z,t)/\lambda_0$, where $n(x,z)$ is the refractive index at location (x,z) in the sample, $\Delta u_z(x,z,t)$ is the difference of the vertical displacements at (x,z) within a time increment t to $t + dt$, and λ_0 is the center wavelength of the OCT light source. From the response pattern in the OCE images Fig. 2b and 2d, recorded with the excitation frequencies 300 Hz and 3600 Hz, respectively, the wavelengths of the elastic waves can be estimated, and the wave speeds (0.63 and 7.03 m/s, respectively) can be obtained by the formula $c = f\lambda$, where c is elastic wave speed, f is frequency, and λ is wavelength. We repeated wave speed measurements at different frequencies, which led to the dispersion curve (frequency-dependent wave speed) of the sample. This experimental dispersion curve was used to determine the estimated shear modulus and shear viscosity via model-based inverse analysis. The details of the model are provided in the next section.

B. Guided Elastic Wave Models

The elastic wavelength plays an important role in the dynamic responses of the soft samples monitored by the OCT microscope. Within the frequency range of 0.1~10 kHz, the wavelength of a longitudinal wave is between 0.1~10 m, which goes beyond the field of view of the OCT microscope. On the other hand, the shear wavelength within this frequency range is three orders smaller, and the wavelength of the surface wave is of the same order with the shear wave. When the wavelength is comparable to the sample thickness, the energy carried by shear and surface waves would interact with the sample boundaries, creating standing wave interference pattern and leading to guided wave propagation. The guided elastic waves can propagate as Love or Lamb waves, whose wave speeds depend on frequency, sample geometry, material properties, and boundary conditions. Therefore, in order to characterize the mechanical properties from the OCE measurements, we developed a planar and a curved guided wave models as shown in Fig. 3 that can predict the dispersive relation given certain sample properties and boundary conditions. For the planar biofilm (Fig. 3a), the layer is assumed to be homogeneous and isotropic with a constant thickness h . The top boundary is exposed in the air and the bottom boundary is supported by a rigid substrate. The coordinates are defined as x in lateral direction and z along depth. The red arrows denoted with L and S and superscripts + and - are partial longitudinal and shear waves traveling along positive and negative z -directions, respectively. For the granular biofilm (Fig. 3b), the model is composed of two homogeneous and isotropic medium layers (radii a and b) and a water half-space as the samples were immersed in their native aquatic solution during the experiments. The two models were solved for solutions that satisfy the boundary conditions and interface continuity of the stresses and displacements. Additional details can be found in Liou *et al.* (2019a, b) [6-7].

III. RESULTS AND DISCUSSION

For the planar biofilm, the dispersion curves obtained from the OCE measurements and the guided wave model are shown in Fig. 4a. The model assumes a constant biofilm thickness (2.5 mm) and uses shear modulus and shear viscosity as free fitting parameters to determine the best fit for the experimental data. The density and the longitudinal wave speed of the biofilm were assumed to be the same as water since the biofilm contains a high percentage of water in its composition (>90%). The best-fit, indicated by the black curve in the figure, suggests that the estimated shear modulus and shear viscosity are 429 Pa and 0.06 Pa-s, respectively. These values fall within the same ranges reported by other studies of biofilms [8].

For the granular biofilm, the elastic wave speed estimated from the OCE measurements are shown in Fig. 4b. Note that for a sample with a curved surface, the elastic waves propagating in this structure belong to circumferential waves. It is known that the granular biofilm may have graded mechanical properties along the depth due to compositional variation; therefore, a layered cylindrical structure may be adapted to simulate the circumferential wave behavior and its dispersive relation in the granular biofilm. Using a cylindrical structure to model a spherical sample may seem questionable; however, we remark

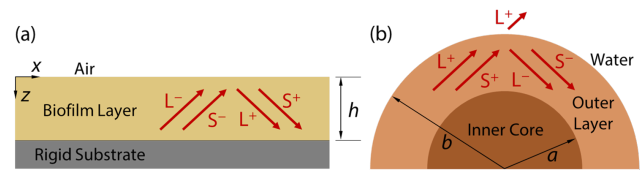


Fig. 3. (a) Planar and (b) curved guided elastic wave models

that if the wave is monitored along the meridian (the big circle) of the sphere, a cylindrical structure with the same curvature of the meridian would be a good approximation and convenient simplification for modeling the circumferential wave traveling along the surface of the granular biofilm [9].

To successfully model the circumferential waves in the granular biofilm, several challenges need to be addressed. The most critical challenge is the lack of knowledge of the mechanical property distribution along the depth. This can be overcome by assuming that the granular biofilm only consists of two layers—the outer layer and the inner core as shown in Fig. 3b—based on the general compositional model [10]. Although the core may contain multiple layers and compositions, it is distanced from the surface where the energy carried by the circumferential waves is weak so that the effect caused by the multiple layers and compositions on the waves may be ignored.

With this model assumption, it is still required to specify (a) the mechanical properties and (b) the sizes of the outer layer and the core. This brings up the need to locally probe the mechanical properties along the sample depth. We developed an approach for local characterization by recording the OCE images at different time delays so that by tracing the phase movement, the local elastic wave speed can be obtained. This approach may be used on cross-sectional cuts from granular biofilms to investigate the depth-dependent mechanical properties.

Instead of applying this approach directly on granular biofilm cuts, we first validated its feasibility on a thick model sample (thickness = 10 mm) made of agarose gel with two concentrations (1.0% and 1.5% weight-to-volume) as shown in Fig. 5a. The large thickness eliminates the effect from the bottom boundary since the wavelengths are much smaller than the thickness. The interface of the two regions was made to have an angle with respect to the incident wave fronts which are normal to the surface so that a gradual compositional transition can be created along the direction of wave propagation. A 2100 Hz voltage signal was applied to the piezoelectric actuator to

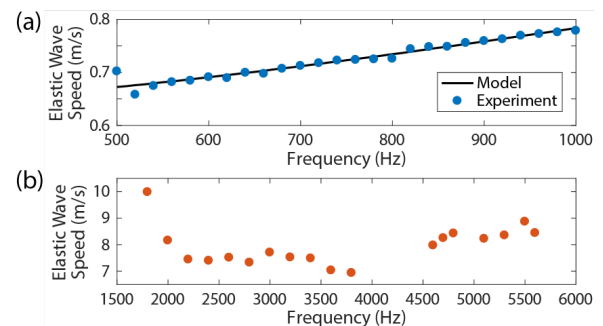


Fig. 4. Frequency-dependent wave speeds obtained from OCE measurements (circular dots) for (a) planar biofilm and (b) granular biofilm. The black curve in (a) is the best-fit dispersion curve calculated by the model.

excite harmonic elastic waves. 21 OCE images were recorded with 25 μ s increment of delay time between each. The phase signals along the wave path indicated by the white dotted line in Fig. 5a near the surface were plotted with respect to the time to create the acoustic B-scan (Fig. 5b). The white dots in Fig. 5b indicate where the phase values are zero. By calculating the local slopes of the white dot tracks, the local wave speed can be estimated as shown in Fig. 5c. The vertical red dotted line indicates the location where the wave path intersects with the agarose interface. The overall trend of the wave speed distribution in Fig. 5c follows the expectation that the elastic wave speed is lower in the left region and higher in the right region based on the agarose concentrations. The local elastic wave speed has more distinct fluctuation within the range close to the interface (3.5~5.5 mm) due to the interference between the incident and reflected waves and the interference created by the transmitted waves at different depths. This region with distinct fluctuation demonstrates a transition zone when the elastic waves encounter compositional change in the medium. This transition zone defines the resolution of the approach to estimate local mechanical properties. In this case, the width of the transition zone is approximately 2 mm, which is of the same order of the wavelength in the right region (2.29 mm). This discovery concludes that the limitation of this approach to probe local variation of mechanical properties depends on the wavelength of the harmonic elastic wave. Therefore, waves at higher frequencies that have shorter wavelengths would be preferable for this application.

IV. CONCLUSION

In this paper, we first demonstrated the OCE measurements and their co-registered OCT images acquired from a planar biofilm and a granular biofilm. The OCE measurements were recorded at different frequencies to obtain the dispersion curves of the samples. Meanwhile, theoretical models with different geometries were established to predict the dispersive relations given certain material properties and boundary conditions. These models use shear modulus and shear viscosity as free fitting parameters to determine the best fits for the experimental data. An example of this inverse modeling was given to estimate the shear modulus and shear viscosity of the planar biofilm. In order to apply the inverse analysis on the granular biofilm, an measurement approach was developed to resolve the mechanical property variation along the depth that is required by the model. This approach was validated on a phantom hydrogel sample, and the result suggests the resolution is limited by the elastic

wavelength. Overall, the studies reported in this paper demonstrate a novel metrology approach to nondestructively characterize the mechanical properties of the biofilms with different geometries. Our future work would aim at completing the mechanical characterization of granular biofilms and exploring the correlation between biofilms' mechanical properties, morphology, compositions, and the environmental conditions.

ACKNOWLEDGMENT

We wish to thank Aqua-Aerobic Systems, Inc. (Rockford, IL, USA) for providing granular biofilms for this work.

REFERENCES

- [1] L. Hall-Stoodley, J. W. Costerton, and P. Stoodley, "Bacterial biofilms: from the Natural environment to infectious diseases," *Nature Reviews Microbiology*, vol. 2, no. 2, pp. 95-108, 2004.
- [2] J. Wilking, T. Angelini, A. Seminara, M. Brenner, and D. Weitz, "Biofilms as complex fluids," *MRS Bulletin*, vol. 36, no. 5, pp. 385-391, 2011.
- [3] H.-C. Flemming, J. Wingender, U. Szewzyk, P. Steinberg, S. A. Rice, and S. Kjelleberg, "Biofilms: an emergent form of bacterial life," *Nature Reviews Microbiology*, vol. 14, no. 9, pp. 563-575, 2016.
- [4] N. Billings, A. Birjiniuk, T. S. Samad, P. S. Doyle, and K. Ribbeck, "Material properties of biofilms—a review of methods for understanding permeability and mechanics," *Reports on Progress in Physics*, vol. 78, no. 3, pp. 036601, 2015.
- [5] B. W. Towler, C. J. Rupp, A. B. Cunningham, and P. Stoodley, "Viscoelastic Properties of a Mixed Culture Biofilm from Rheometer Creep Analysis," *Biofouling*, vol. 19, no. 5, pp. 279-285, 2003.
- [6] H.-C. Liou, F. Sabba, A. I. Packman, G. Wells, and O. Balogun, "Nondestructive characterization of soft materials and biofilms by measurement of guided elastic wave propagation using optical coherence elastography," *Soft Matter*, vol. 15, no. 4, pp. 575-586, 2019a.
- [7] H.-C. Liou, F. Sabba, A. I. Packman, A. Rosenthal, G. Wells, and O. Balogun, "Towards mechanical characterization of granular biofilms by optical coherence elastography measurements of circumferential elastic waves," *Soft Matter*, vol. 15, no. 28, pp. 5562-5573, 2019b.
- [8] B. W. Peterson, Y. He, Y. Ren, A. Zerdoum, M. R. Libera, P. K. Sharma, A.-J. van Winkelhoff, D. Neut, P. Stoodley, H. C. van der Mei, and H. J. Busscher, "Viscoelasticity of biofilms and their recalcitrance to mechanical and chemical challenges," *FEMS Microbiology Reviews*, vol. 39, no. 2, pp. 234-245, 2015.
- [9] S. Towfighi and T. Kundu, "Elastic wave propagation in anisotropic spherical curved plates," *International Journal of Solids and Structures*, vol. 40, no. 20, pp. 5495-5510, 2003.
- [10] X.-W. Liu, G.-P. Sheng, and H.-Q. Yu, "Physicochemical characteristics of microbial granules," *Biotechnology Advances*, vol. 27, no. 6, pp. 1061-1070, 2009.

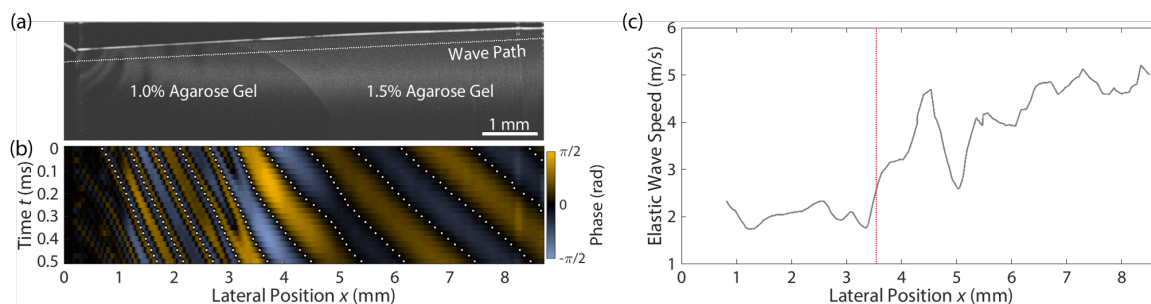


Fig. 5. (a) OCT image of the two-layered agarose gel sample, (b) acoustic B-scan of the 2100 Hz elastic wave, and (c) local elastic wave speed estimated from (b).